THE ASTROPHYSICAL JOURNAL, 457:529–541, 1996 February 1

GRAVITATIONAL LENSING OF QUASI-STELLAR OBJECTS BY THEIR DAMPED Lyα ABSORBERS

MATTHIAS BARTELMANN[1] AND ABRAHAM LOEB
Harvard-Smithsonian Center for Astrophysics, 60 Garden Street, Cambridge, MA 02138
Received 1995 May 18; accepted 1995 August 9

ABSTRACT

Damped Lyα absorbers are believed to be associated with galactic disks. We show that gravitational lensing can therefore affect the statistics of these systems. First, the magnification bias due to lensing raises faint QSOs above a given magnitude threshold and thereby enhances the probability for observing damped absorption systems. Second, the bending of light rays from the source effectively limits the minimum impact parameter of the line of sight relative to the center of the absorber, thus providing an upper cutoff to the observed neutral hydrogen (H I) column density. The ray bending also reduces a possible obscuration of the QSO by dust. The combination of the lensing effects yields a pronounced peak in the observed abundance of absorbers with high column densities ($\gtrsim 2 \times 10^{21}$ cm^{-2}) and low redshifts ($z_{\rm abs} \lesssim 1$) in the spectra of bright QSOs ($B \lesssim 18$ mag) with redshifts $z_{\rm QSO} \gtrsim 2$. The inferred value of the cosmological density parameter of neutral hydrogen, $\Omega_{\rm H\,I}$, increases with increasing redshift and luminosity of the sources even if the true H I density remains constant. This trend is consistent with the observed evolution of $\Omega_{\rm H\,I}(z)$. Damped Lyα absorbers with column densities $\gtrsim 10^{21}$ cm^{-2} and redshifts $0.5 \lesssim z_{\rm abs} \lesssim 1$ are reliable flags for lensed QSOs with a close pair of images separated by $\sim 0\farcs3 \times (v_c/220$ km s$^{-1})^2$, where v_c is the rotational velocity of the lens. Detection of these gravitational lensing signatures with the *Hubble Space Telescope* can be used to constrain the depth of the absorber potential wells and the cosmological constant.

Subject headings: cosmology: theory — gravitational lensing — large-scale structure of universe — quasars: absorption lines

1. INTRODUCTION

Most of the neutral hydrogen probed by QSO absorption spectra is traced by damped Lyα absorption lines, corresponding to H I column densities of 10^{20}–10^{22} cm^{-2} (see, e.g., Wolfe 1988; Lanzetta, Wolfe, & Turnshek 1995). The high H I content and the cosmological abundance of damped Lyα systems suggest that they are associated with galactic disks (Wolfe 1988). Direct evidence for this identification is indeed provided by a wealth of observational facts. First, recent images of QSOs exhibiting damped Lyα systems in their spectra show related galaxies (cf. Steidel et al. 1994, 1995). Second, abundant heavy element absorption lines at low-ionization stages are frequently associated with damped Lyα absorption systems (Turnshek et al. 1989; Wolfe et al. 1993; Pettini et al. 1994). Third, the velocity field traced by these metal lines relative to the damped Lyα line is consistent with typical galactic rotation velocities, if the damped component is associated with a galactic disk while the metal-line systems are embedded in a surrounding halo (Lanzetta & Bowen 1992; Lu et al. 1993; Turnshek & Bohlin 1993; Lu & Wolfe 1994). Fourth, observations of redshifted 21 cm absorption and emission indicate disklike structures that extend across galactic dimensions (Briggs et al. 1989; Wolfe et al. 1992b). Fifth, Faraday rotation observations of QSOs with damped Lyα systems are consistent with the existence of micro-Gauss magnetic fields in the absorbers, of the same magnitude as detected in nearby disk galaxies (Welter, Perry, & Kronberg 1984; Wolfe, Lanzetta, & Oren 1992a; Kronberg, Perry, & Zukowski 1992; however, note the caveat in Perry, Watson, & Kronberg 1993). Based on these clues, we adopt the view that damped Lyα absorption arises from neutral hydrogen in ordinary disk galaxies.

The characteristic H I density profiles of nearby spiral galaxies can be used to get a rough estimate of the impact parameter of lines of sight to QSOs relative to the centers of damped Lyα absorbers. Typical H I column densities of $\gtrsim 2 \times 10^{20}$ cm^{-2} imply impact parameters $\lesssim 15\ h^{-1}$ kpc (Broeils & van Woerden 1994). This characteristic separation is indeed confirmed by direct imaging (Steidel et al. 1994, 1995). Geometrically, the absorbing disk can be intersected through a variety of impact parameters, with some lines of sight passing very close to the center of the absorber. If the damped systems resemble nearby disk galaxies, then the effects of gravitational lensing are strong and inevitable for lines of sight passing less than a few kiloparsecs from the absorber center, where the H I column density is high. The statistics of high column density systems would then be marked by a pronounced lensing signature.

Gravitational lensing gives rise to two distinct effects. First, it magnifies the flux of the background QSO population and thus increases the number of sources above a given magnitude limit (see, e.g., Narayan & Wallington 1993; Schneider, Ehlers, & Falco 1992; Schneider 1992). The magnification bias tends to artificially increase the fraction of QSOs which show damped Lyα systems. Second, the bending of light rays effectively limits the minimum impact parameter of the line of sight toward the QSO relative to the absorber center and therefore provides an upper cutoff to the column density distribution of damped Lyα absorbers. The strength of these lensing effects depends on the depth of the gravitational potential well of the absorbers and on the underlying cosmology.

[1] Max-Planck-Institut für Astrophysik, Postfach 1523, D-85740 Garching, Germany.

Within the framework of Friedmann-Lemaître cosmological models, a possible nonzero cosmological constant has a strong influence on the statistics of lensing events (Turner 1990; Kochanek 1992).

The magnification bias is most pronounced for high column density absorbers in the spectra of bright QSOs. Systems specified by these two requirements are particularly easy to observe, given a sufficiently large sample of QSOs. The search for the lensing signature requires space-based observations because lensing is primarily effective for absorbers at redshifts $z_{\rm abs} \sim 0.5$–1 and sources at $z_{\rm QSO} \gtrsim 2$. Unfortunately, existing surveys of damped Lyα systems using ground-based and *IUE* observations (see, e.g., Lanzetta et al. 1995, and references therein) do not cover simultaneously the redshift ranges for absorbers and sources which are optimal for lensing. However, it should be straightforward to extend these surveys and to design an optimal search strategy that will probe the lensing signatures predicted in this paper through future observations with the *Hubble Space Telescope*. If gravitational lensing indeed occurs in damped Lyα absorption systems, one would expect the formation of multiple QSO images, especially in high column density systems. It is, however, not surprising that multiple images were not resolved in such systems in the past, because the characteristic image splitting provided by spiral galaxies is $\lesssim 0\farcs3$. On the other hand, the only known lens system with an image separation as small as $0\farcs34$, B0218+357 (O'Dea et al. 1992; Patnaik et al. 1993), shows 21 cm absorption (Carilli, Rupen, & Yanny 1993), which indicates a high H I column density consistent with our expectations. Damped Lyα absorption at a fairly low column density, $\sim 7 \times 10^{19}$ cm^{-2}, was observed in the spectrum of both images of QSO 0957+561 (Turnshek & Bohlin 1993), but in that case the large angular separation of $\sim 6''$ is caused by an intervening galaxy cluster.

The magnification bias also affects estimates for the value of the cosmological density parameter of neutral hydrogen in damped Lyα systems, $\Omega_{\rm H\,I}$. It has recently been argued that the observed decline of $\Omega_{\rm H\,I}$ between $z \sim 3.5$ and the present time (White, Kinney, & Becker 1993; Bahcall et al. 1993; Lanzetta et al. 1995) is a natural consequence of the conversion of gas into stars in disk galaxies (Kauffmann & Charlot 1994; Lanzetta et al. 1995). Here, we examine the effect of lensing on the estimate of $\Omega_{\rm H\,I}(z)$. Although high column density systems are rare, their contribution to the estimate of $\Omega_{\rm H\,I}$ is dominant, and so the lensing effect on their apparent abundance can change the apparent value of $\Omega_{\rm H\,I}$ considerably. In particular, we show that the inferred value of $\Omega_{\rm H\,I}$ should generically decline with decreasing source redshift even if the true H I density in the absorbers remains constant. This apparent evolution results from the change in the efficiency of lensing with redshift.

Previously, Krolik & Kwan (1979) investigated the importance of lensing in general absorption systems and argued that multiple imaging would occur only in a very small subset of all systems. Indeed, Ikeuchi & Turner (1991) concluded that Lyα forest clouds most likely do not cause any significant gravitational lensing effects. Thomas & Webster (1990) used a simplified model to examine the influence of the magnification bias on the observed statistics of metal absorption lines in QSO spectra. They concluded that the redshift distribution of the absorbers is at most weakly affected by lensing. Our study focuses on damped Lyα absorption systems which are more likely to arise at small impact parameters where lensing is expected to be stronger. Moreover, we address additional statistical properties of the absorbers which are more sensitive to gravitational lensing.

The outline of this paper is as follows. In § 2 we develop the formalism required to investigate the various signatures of gravitational lensing. We adopt the simplest model for damped Lyα absorbers, assuming no cosmological evolution in their H I density profiles, which we model according to observed profiles in nearby disk galaxies. This simple model provides a good fit to the observed column density distribution of the damped Lyα systems. Moreover, the strongest lensing signature is expected for absorbers at low redshift ($z_{\rm abs} \sim 0.5$), where evolutionary effects due to mergers or accretion should be weak (Tóth & Ostriker 1992; Zaritsky 1995). The numerical results for the various lensing signatures are presented in § 3. Finally, § 4 summarizes our main conclusions.

2. FORMALISM

2.1. *Parameterization of the Absorber Population*

In the following subsections, we calculate the probability that intervening disk galaxies produce damped Lyα absorption and simultaneously magnify the background QSOs whose spectra show the absorption lines. We assume that the absorber population can be parameterized by the Schechter luminosity function (Schechter 1976),

$$\Phi(l)dl = \Phi_* \, l^s \exp(-l) dl \,, \tag{2.1}$$

where $l \equiv (L/L_*)$ is the luminosity in units of the luminosity scale L_*, and where, for spiral galaxies (Marzke et al. 1994)

$$\Phi_* = 1.5 \times 10^{-2} \, h^3 \ {\rm Mpc}^{-3} \,, \qquad s = -0.81 \,. \tag{2.2}$$

As usual, h is the Hubble constant H_0 in units of 100 km s^{-1} Mpc^{-1}. The geometry of the absorber system is shown in Figure 1.

We further assume that each light ray which passes an intervening absorption system face-on within a radius $R_{\rm H}(N')$ from its center shows damped Lyα absorption with a column density equal to or greater than N'. Following common practice (e.g., Lanzetta et al. 1991; Wolfe et al. 1986), we take $R_{\rm H}(N')$ to be proportional to the optical radius R, and the optical radius to be proportional to some power t of the luminosity of the system,

$$R_{\rm H}(N') = f_{\rm H}(N') R_* \, l^t \,, \tag{2.3}$$

where R_* is the optical radius of an L_* galaxy. Observations suggest the values (e.g., Holmberg 1975; Peterson, Strom, & Strom 1979; Broeils & van Woerden 1994)

$$R_* \approx 11 \ h^{-1} \ {\rm kpc} \,, \qquad t \approx 0.4 \,. \tag{2.4}$$

Measurements of the surface density of neutral hydrogen in local disk galaxies (e.g., Broeils & van Woerden 1994) suggest that the surface density of neutral hydrogen is well fitted by an exponential function of radius. Figure 8*b* of Broeils & van Woerden (1994)

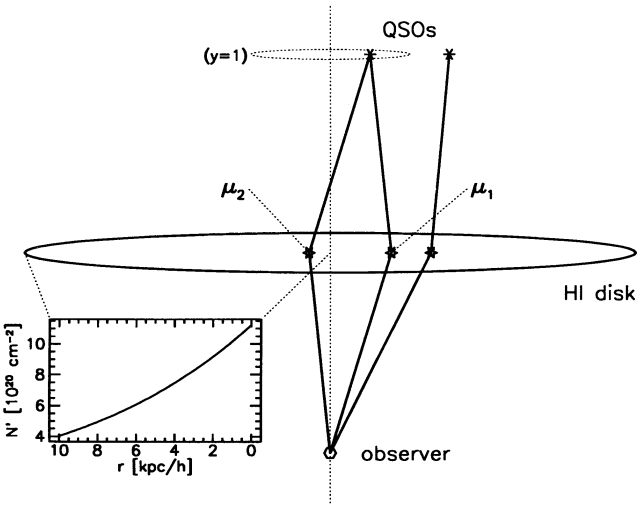

FIG. 1.—Schematic illustration of the lensing geometry. QSOs in the source plane are either multiply or singly imaged, depending on their distance from the optical axis. The two corresponding regions in the source plane are separated by the dotted curve, marked $y = 1$. Light rays are magnified by the lens on their way to the observer. The magnification factors, μ_1 and μ_2, of the two images of the central QSO are indicated for further reference. The inserted figure displays the face-on hydrogen column density as a function of radius in the H I disk.

shows average H I profiles such that

$$f_{\rm H}(N') = \frac{3}{2} - 2\log\left(\frac{N'}{2\times 10^{20}\ {\rm cm}^{-2}}\right) \tag{2.5}$$

describes reasonably well the average disk radius within which the neutral-hydrogen column density exceeds N'. Note that N' is the face-on column density of the neutral hydrogen disk. If the disk is inclined by an angle θ relative to the line of sight, the observed column density is $N = N'/\cos\theta$. We neglect the finite scale height of the hydrogen disk, which is typically smaller by 1–2 orders of magnitude than the disk radius. The geometrical cross section $\sigma_{{\rm Ly}\alpha}(N)$ of a disk inside of which the observed column density exceeds N is obtained by averaging over all inclination angles,

$$\sigma_{{\rm Ly}\alpha}(N) = \pi R^2 \int_0^1 d\gamma f_{\rm H}^2(N\gamma)\gamma {\rm H}(\gamma - \gamma_0)\,, \tag{2.6}$$

where $\gamma \equiv \cos\theta$, and the Heaviside step function ${\rm H}(\gamma - \gamma_0)$ accounts for the fact that very high column densities can be observed only in disks which are inclined by an angle $\theta \geq \theta_0$, with

$$\gamma_0 \equiv \cos\theta_0 = \min\left[1,\ 10^{3/4}\left(\frac{2\times 10^{20}\ {\rm cm}^{-2}}{N}\right)\right]. \tag{2.7}$$

Evaluating the average in equation (2.6), we obtain

$$\sigma_{{\rm Ly}\alpha}(N) = \pi R^2 \langle f_{\rm H}^2(N)\rangle\,, \tag{2.8}$$

where

$$\langle f_{\rm H}^2(N)\rangle^{1/2} = \frac{\gamma_0}{2}\left[f_{\rm H}^2(N) - 2f_{\rm H}(N)\frac{2\ln\gamma_0 - 1}{\ln 10} + \frac{2}{\ln^2 10}(1 - 2\ln\gamma_0 + 2\ln^2\gamma_0)\right]^{1/2}. \tag{2.9}$$

We define the angle-averaged disk radius for absorption with column density $\geq N$ by

$$\langle R_{\rm H}(N)\rangle = R\langle f_{\rm H}^2(N)\rangle^{1/2}\,. \tag{2.10}$$

We model the lensing properties of the intervening systems as singular isothermal spheres, assuming that these systems resemble galactic disks with flat rotation curves which are embedded in spherical halos. Such systems are the simplest to consider, as they are characterized by only one parameter, viz. their one-dimensional velocity dispersion, σ_v. *HST* observations of bulges of spiral galaxies show no indication for cores, i.e., central regions in which the surface brightness is constant (Tremaine et al. 1996). Similarly, models for observed gravitational lens systems indicate that the density profiles of the lenses are either singular or have very small core radii $\lesssim 200$ pc (Kochanek 1991). These are mostly elliptical galaxies, but where the lensing object is a spiral galaxy, e.g., in QSO 2237+0305 (Rix, Schneider, & Bahcall 1992) or in B0218+357 (O'Dea et al. 1992; Patnaik et al. 1993), the image configuration also argues for small or singular cores. Singular cores do not necessarily imply flat stellar rotation curves all the way into the centers of spiral galaxies because the stellar velocity distributions may acquire large dispersions inside bulges and may not even be axisymmetric due to bars.

Assuming a circular rotational velocity of $v_{c,*} = 220$ km s^{-1} for an L_* galaxy (e.g., Peebles 1993; Aaronson, Huchra, & Mould 1979), we get

$$\sigma_{v,*} = \frac{v_{c,*}}{\sqrt{2}} \approx 160 \text{ km s}^{-1} . \tag{2.11}$$

The rotational velocity, and hence the velocity dispersion, are related to the luminosity through the Tully-Fisher relation (Tully & Fisher 1977),

$$\sigma_v = l^{1/\alpha}\sigma_{v,*} . \tag{2.12}$$

The Tully-Fisher exponent α depends on the waveband where the observations are taken; it ranges from $\alpha \approx 2$ in the blue to $\alpha \approx 4$ in the infrared (see Strauss & Willick 1995, and references therein).

2.2. *Probability for Damped Lyα Absorption*

Ignoring gravitational lensing, the probability for a QSO to exhibit damped Lyα absorption in its spectrum can be calculated by dividing the physical path length surveyed for absorption by the mean free path between subsequent absorptions,

$$P_{\text{Ly}\alpha}(N) = n_{\text{Ly}\alpha}\sigma_{\text{Ly}\alpha}(N)\Delta X , \tag{2.13}$$

where $n_{\text{Ly}\alpha}$ is the spatial number density of absorbers and $\sigma_{\text{Ly}\alpha}(N)$ is their individual cross section for damped Lyα absorption with a column density $\geq N$, given by equation (2.8). Integrating over galaxy luminosities we find

$$n_{\text{Ly}\alpha}\sigma_{\text{Ly}\alpha}(N) = \Phi_*\Gamma(1 + s + 2t)\pi R_*^2\langle f_{\text{H}}^2(N)\rangle , \tag{2.14}$$

where the gamma function results from the Schechter luminosity function, taking the luminosity dependence of R into account. The physical path length between redshifts z_1 and z_2 is given by the absorption distance difference,

$$\Delta X(z_1, z_2) = \int_{z_1}^{z_2} dz(1 + z)^3 \left| \frac{c\,dt}{dz} \right| , \tag{2.15}$$

where the factor $(1 + z)^3$ accounts for the change in the galaxy density due to the cosmological expansion. The proper-distance interval $|c\,dt|$ depends on the cosmological parameters,

$$|c\,dt| = \frac{c}{H_0}\frac{dz}{1 + z}\frac{1}{\sqrt{\Omega_0(1 + z)^3 + (1 - \Omega_0 - \Omega_\Lambda)(1 + z)^2 + \Omega_\Lambda}} , \tag{2.16}$$

where Ω_0 is the present-day density parameter, and Ω_Λ is the cosmological constant. Combining the last four equations, we obtain

$$P_{\text{Ly}\alpha}(z_1, z_2, N) = \Phi_*\Gamma(1 + s + 2t)\pi R_*^2\langle f_{\text{H}}^2(N)\rangle \int_{z_1}^{z_2} dz(1 + z)^3 \left| \frac{c\,dt}{dz} \right| \tag{2.17}$$

(see also Bahcall & Peebles 1969; Burbidge et al. 1977). Note that $P_{\text{Ly}\alpha}(z_1, z_2, N)$ is independent of the Hubble constant.

This equation changes considerably due to the magnification bias when gravitational lensing is taken into account. The derivation of the absorption probability can then be split into two steps; one to calculate the probability for magnification, and the second to convolve the magnification probability with the QSO number counts.

We adopt the conventional description of gravitational lensing (e.g., Schneider et al. 1992). The optical axis of the lens system is defined by the positions of the observer and the center of the lens, and the lens and source planes are constructed orthogonal to the optical axis at the redshifts z and z_s of the lens and the source, respectively. Later, we shall refer to z and z_s by the redshifts of the absorbers, z_{abs}, and the QSOs, z_{QSO}. The lens plane constitutes the observer's sky in the vicinity of the lens. We normalize the coordinates in the lens plane by the length scale appropriate for singular isothermal spheres,

$$\xi_0 \equiv 4\pi\left(\frac{\sigma_v}{c}\right)^2 \frac{c}{H_0}\frac{r_{\text{d}}\, r_{\text{ds}}}{r_{\text{s}}} \equiv 4\pi\left(\frac{\sigma_v}{c}\right)^2 \frac{c}{H_0}\, d(z, z_{\text{s}}) , \tag{2.18}$$

where $r_{\text{d}}, r_{\text{s}}$, and r_{ds} are the angular diameter distances from the observer to the lens (deflector) and the source planes, and from the lens to the source plane, respectively, in units of the Hubble length (c/H_0). For a detailed description of the lensing properties of singular isothermal spheres, see § 8.1 of Schneider et al. (1992). Coordinates in the source plane are correspondingly scaled by the projection of ξ_0 from the lens onto the source plane. Using equation (2.12), the length scale ξ_0 can be written as

$$\xi_0 = 4\pi\left(\frac{\sigma_{v,*}}{c}\right)^2 \frac{c}{H_0}\, d(z, z_{\text{s}})l^{2/\alpha} \equiv \frac{c}{H_0}\,\theta_*\, d(z, z_{\text{s}})l^{2/\alpha} . \tag{2.19}$$

We denote the scaled coordinates in the lens and source planes by x and y, respectively. Then, sources with $y \leq 1$ have two images at $x = y \pm 1$, while sources outside $y = 1$ have a single image at $x = y + 1$. The total magnification of a point source is

$$\mu = \begin{cases} 2/y & (y \leq 1) \\ 1 + 1/y & (\text{otherwise}) \end{cases} . \tag{2.20}$$

If a source is multiply imaged, and if the multiple images are not resolved when the spectrum of the source is taken, then the damped Lyα absorption of the two superposed spectra is dominated by that of the brighter image that is formed at the larger impact parameter, $x = y + 1$. If the lens is nonsingular, a third image arises for sufficiently small y at the center of the lens. Its

magnification, however, scales with the square of the core radius x_c in units of the length scale ξ_0 for small x_c and can thus safely be neglected in this study. In order to get damped Lyα absorption with column density $\geq N$ in the composite spectrum, the outer image of the source must therefore lie at a sufficiently small impact parameter. This is equivalent to the requirement

$$y \leq y_H(N) = x_H(N) - 1 = \frac{\langle R_H(N) \rangle}{\xi_0} - 1 . \tag{2.21}$$

Inserting equations (2.3), (2.10), and (2.19) into equation (2.21), we obtain

$$y_H(z, z_s, N) = \frac{H_0 R_* \langle f_H^2(N) \rangle^{1/2}}{c\theta_* d(z, z_s)} l^{t-2/\alpha} - 1 . \tag{2.22}$$

For reasonable choices of t and α, $(t - 2/\alpha) \approx 0$, so that $y_H(z, z_s, N)$ depends only weakly on l. In the following, we shall assume that $y_H(z, z_s, N)$ is independent of l since this simplifies our discussion considerably.

The dimensionless cross section of the intervening system for magnifying a point source by more than a factor μ and causing damped Lyα absorption with a column density of $\geq N$ is defined to be the corresponding area in the source plane within which a point source has to lie, normalized by the square of the length scale in the source plane. For the singular isothermal sphere, the cross section is given by (cf. Schneider et al. 1992)

$$\sigma(z, z_s, N; \mu) = \begin{cases} 4\pi/\mu^2 & [\mu \geq 2/y_H(z, z_s, N)] \\ \pi y_H^2(z, z_s, N) & \text{(otherwise)} \end{cases} , \tag{2.23}$$

if $y_H(z, z_s, N) \leq 1$, or by

$$\sigma(z, z_s, N; \mu) = \begin{cases} 4\pi/\mu^2 & (\mu \geq 2) \\ \pi/(\mu - 1)^2 & [2 > \mu \geq 1 + 1/y_H(z, z_s, N)] \\ \pi y_H^2(z, z_s, N) & \text{(otherwise)} \end{cases} , \tag{2.24}$$

if $y_H(z, z_s, N) > 1$.

The probability for a QSO to be magnified by more than μ and at the same time to show damped Lyα absorption with column density $\geq N$ in its spectrum can now be found by calculating the fraction of the total area of the source sphere covered by the appropriate cross sections of the lens population. Implicitly, this assumes that lenses and QSOs are physically uncorrelated and that the cross sections do not significantly overlap; both of these assumptions are well justified. Integrating over source luminosity and redshift between redshifts z_1 and $z_2 \leq z_s$, we obtain the probability that a QSO at redshift z_s shows damped Lyα absorption with column density $\geq N$ and is magnified by a factor $\geq \mu$ by lenses in the redshift interval $z_1 \leq z \leq z_2$,

$$P'_{GL}(z_1, z_2, z_s, N; \mu) = \left(\frac{c}{H_0}\right)^2 \Phi_* \theta_*^2 \Gamma\left(1 + s + \frac{4}{\alpha}\right) \int_{z_1}^{z_2} dz\, d^2(z, z_s)(1 + z)^3 \left| \frac{c\, dt}{dz} \right| \sigma(z, z_s, N; \mu) . \tag{2.25}$$

As in equation (2.14), the gamma function results from integrating over luminosity, assuming that the dimensionless magnification cross section is independent of l.

Equation (2.17) should be a limiting case of equation (2.25) in the sense that if we disregard lensing, equation (2.25) should equal equation (2.17). In fact, if we allow for any magnification factor by setting $\mu \to 1$, the cross section is limited by the column density requirement only, and we obtain from equations (2.23) or (2.24)

$$\sigma(z, z_s, N; \mu) \to \pi y_H^2(z, z_s, N) . \tag{2.26}$$

If $\mu \to 1$, we further have $y_H(z, z_s, N) \gg 1$, and thus

$$\sigma(z, z_s, N; \mu) \to \pi \langle f_H^2(N) \rangle R_*^2 \left[\frac{H_0}{c\theta_* d(z, z_s)}\right]^2 . \tag{2.27}$$

Inserting this into equation (2.25), we obtain

$$P'_{GL}(z_1, z_2, z_s, N; \mu) \to \Phi_* \Gamma\left(1 + s + \frac{4}{\alpha}\right) \pi R_*^2 \langle f_H^2(N) \rangle \int_{z_1}^{z_2} dz (1 + z)^3 \left| \frac{c\, dt}{dz} \right| , \tag{2.28}$$

which is identical with equation (2.17) provided that $t \approx 2/\alpha$, as we have assumed before for simplicity.

Let now $(dN_{QSO}/dS)(S)dS$ be the intrinsic number of QSOs at redshift z_s with flux between S and $S + dS$. Due to the magnification bias, the observed number of QSOs with flux greater than S which show damped Lyα absorption with column density $\geq N$ between redshifts z_1 and z_2 is given by

$$N'_{QSO}(S) = \int_0^\infty dS' P'_{GL}\left(z_1, z_2, z_s, N; \frac{S}{S'}\right) \frac{dN_{QSO}}{dS}(S') \tag{2.29}$$

(see, e.g. Schneider et al. 1992; Narayan & Wallington 1993). Therefore, the probability for a QSO at redshift z_s to be detected with a flux greater than S and to show damped Lyα absorption with column density greater than N is given by

$$P_{GL}(z_1, z_2, z_s, N; S) = \frac{1}{N_{QSO}(S)} \int_0^\infty dS' P'_{GL}\left(z_1, z_2, z_s, N; \frac{S}{S'}\right) \frac{dN_{QSO}}{dS}(S') . \tag{2.30}$$

If we disregard gravitational lensing, $P_{GL}(z_1, z_2, z_s, N; S)$ reduces to equation (2.17) and becomes independent of the QSO flux S.

The intrinsic QSO number counts are well modeled by a broken power law (e.g., Boyle, Shanks, & Peterson 1988, Hartwick & Schade 1990),

$$\frac{dN_{\rm QSO}}{dS}(S) = \begin{cases} S^{-a} & (S \le S_0) \\ S^{-b} & (\text{otherwise}) \end{cases}, \tag{2.31}$$

where $a = 1.64$ and $b = 3.52$ provide a reasonable fit to observational data (Pei 1995). The break luminosity S_0 corresponds to an apparent QSO magnitude of $B \approx 19$ (Boyle et al. 1988; Hartwick & Schade 1990).

2.3. *Inferred Properties of Damped Lyα Absorbers*

One of the goals of observing Lyα absorbers is to infer the amount of neutral hydrogen in the universe and thereby to study the history of systems which contain neutral hydrogen. An intermediate step in this calculation is to derive the column density distribution function $f(N)$ of the absorbers, which is defined to be the number of absorbers with column density within dN of N per unit absorption distance dX. Using the definition of the absorption distance, the probability without lensing, equation (2.17), can be written as

$$P_{\rm Ly\alpha}(z_1, z_2, N) = \Phi_* \Gamma(1 + s + 2t)\pi R_*^2 \langle f_{\rm H}^2(N)\rangle [X(z_2) - X(z_1)] . \tag{2.32}$$

If among a sample of q QSOs l damped Lyα absorbers are found within a column density range of ΔN around N, and if the absorption distance surveyed per QSO is $\Delta X(z_1, z_2)$, then the column density distribution inferred from these observations is given by

$$f(N)dN\,dX = \frac{c}{H_0}\frac{l}{q\Delta X(z_1, z_2)\Delta N}\,dN\,dX . \tag{2.33}$$

Since (l/q) approximates the probability for a QSO to show the specified absorption, we can write

$$f(N) = \frac{c}{H_0}\frac{1}{\Delta X(z_1, z_2)}\left|\frac{\partial P(z_1, z_2, N)}{\partial N}\right| . \tag{2.34}$$

Note that $f(N)$ scales linearly with the value of the Hubble constant, because P is independent of H_0 and ΔX is proportional to H_0^{-1}. Ignoring gravitational lensing, equation (2.32) can be substituted into equation (2.34) to give

$$f_{\rm Ly\alpha}(N) = \frac{c}{H_0}\Phi_* \Gamma(1 + s + 2t)\pi R_*^2 \left|\frac{\partial \langle f_{\rm H}^2(N)\rangle}{\partial N}\right| . \tag{2.35}$$

This result is independent of the QSO redshift, the QSO flux, and the redshift interval surveyed for damped Lyα absorption. If, however, gravitational lensing is taken into account, equation (2.34) reads

$$f_{\rm GL}(z_1, z_2, z_s, S; N) = \frac{c}{H_0}\frac{1}{\Delta X(z_1, z_2)}\left|\frac{\partial P_{\rm GL}(z_1, z_2, z_s, N; S)}{\partial N}\right| . \tag{2.36}$$

The resulting column density distribution depends on the redshifts selected, the cosmological parameters, and, in particular, on the QSO flux S because of the magnification bias.

Given $f(N)$, the inferred comoving density of neutral hydrogen in systems with column densities of $N_1 \le N \le N_2$, normalized by the present critical density, is found to be

$$\Omega_{\rm H\,I}(N_1, N_2) = \frac{H_0}{c}\frac{\bar{m}}{\rho_{c,0}}\int_{N_1}^{N_2} dN N f(N) , \tag{2.37}$$

where $\bar{m}$ is the mean molecular mass per proton, and $\rho_{c,0}$ is the present-day closure density,

$$\rho_{c,0} = \frac{3H_0^2}{8\pi G} . \tag{2.38}$$

The lower integration bound is fixed by the requirement that the absorption be damped, i.e., $N_1 \sim 10^{20}$ cm^{-2}. In principle, the choice of N_2 is arbitrary, but in existing surveys it is limited to $N_2 \lesssim 10^{22}$ cm^{-2}. Since $f(N)$ scales linearly with the Hubble constant, $\Omega_{\rm H\,I}$ is independent of H_0.

The fact that $f(N)$ depends on the redshifts chosen and the QSO flux when gravitational lensing is taken into account implies that the inferred value of $\Omega_{\rm H\,I}$ depends on these parameters.

3. RESULTS

Based on the formalism developed in § 2, we now consider quantitatively the characteristic signatures imprinted by gravitational lensing upon quantities inferred from studies of damped Lyα absorption systems. We begin with the column density distribution function, $f(N)$. Figure 2 shows $Nf(N)$ for two choices for the absorber–redshift interval and for three cosmological models. We fix

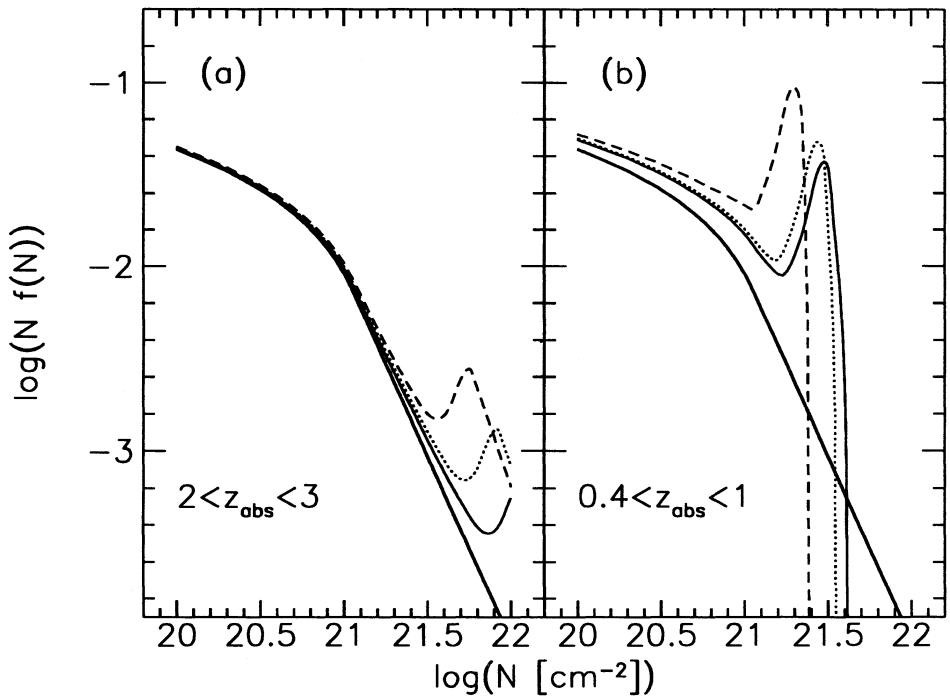

FIG. 2.—Column density distribution of damped Lyα absorbers per logarithmic column density interval, $Nf(N)$, for $H_0 = 50$ km s^{-1} Mpc^{-1}. The integral of this function is proportional to the cosmological density of neutral hydrogen, $\Omega_{H\,I}$. The heavy curve in both panels displays $Nf(N)$ without the influence of gravitational lensing. The three other curves were calculated for three different cosmological models, taking gravitational lensing into account. The cosmological model parameters are $\Omega_0 = 1$, $\Omega_\Lambda = 0$ (*solid line*); $\Omega_0 = 0.2$, $\Omega_\Lambda = 0$ (*dotted line*); and $\Omega_0 = 0.2$, $\Omega_\Lambda = 0.8$ (*dashed line*). In both panels, the QSO redshift is fixed at $z_{QSO} = 3$. In (*a*), the redshift interval for the absorbers is $2 \le z_{abs} \le 3$, and in (*b*), $0.4 \le z_{abs} \le 1$. While the influence of lensing is weak for high-redshift absorbers, a pronounced peak followed by a sharp cutoff arises for low-redshift absorbers. The QSO magnitude threshold is $B = 17$. We ignore the effect of possible obscuration by dust.

the QSO redshift at $z_{QSO} = 3$ and consider the absorber–redshift intervals of $2 \le z_{abs} \le 3$ (Fig. 2*a*) and $0.4 \le z_{abs} \le 1$ (Fig. 2*b*). The heavy line in both panels of Figure 2 shows $Nf(N)$, ignoring gravitational lensing, and the three additional curves display the effect of lensing for the cosmological models $\Omega_0 = 1$, $\Omega_\Lambda = 0$ (*solid line*); $\Omega_0 = 0.2$, $\Omega_\Lambda = 0$ (*dotted line*); and $\Omega_0 = 0.2$, $\Omega_\Lambda = 0.8$ (*dashed line*).

The observed column density distribution of Lyα absorbers can be well fitted by a power law over a broad range of column densities, $f(N) \propto N^\beta$ with $\beta = -1.7 \pm 0.2$ (Tytler 1987; Lanzetta et al. 1991). Our results for $f(N)$ reproduce this power-law behavior well for $N \lesssim 10^{21}$ cm^{-2}, where the effect of lensing is weak. This indicates that our modeling of the neutral hydrogen profiles in galactic disks is reasonable.

For high-redshift absorbers ($z_{abs} \lesssim z_{QSO}$), $Nf(N)$ rises to a peak around $N \sim 10^{22}$ cm^{-2} and then declines sharply at larger N. The peak at $N \sim 10^{22}$ cm^{-2} is due to the magnification bias, because lines of sight passing through higher column densities experience higher magnifications on average. The magnification bias is weak for high-redshift absorbers (cf. Fig. 2*a*). However, for low-redshift absorbers and high-redshift QSOs, lensing by the absorbers is much more efficient, so that the peak in $Nf(N)$, produced by the magnification bias, is much more pronounced (cf. Fig. 2*b*). For column densities beyond the peak location, $Nf(N)$ sharply cuts off. If the QSO is singly imaged, the ray bending due to the lens increases the impact parameter of the QSO image compared to the case of inefficient lensing. If the QSO is multiply imaged, the brighter image whose spectrum dominates the absorption feature is also formed at a larger distance from the center of the lens than in the unlensed case. Thus, the lens prevents the light of the dominant image from passing through the highest column density regions of the galactic disks, so that the highest column densities cannot be traversed by the dominant fraction of the QSO light.

Since $y_H \ge 0$, equation (2.21) requires that

$$\xi_0 \le \langle R_H(N) \rangle \tag{3.1}$$

for such lenses which contribute to damped Lyα absorption with a column density $\ge N$. This implies that the maximum lensing efficiency of the absorbers is achieved for a column density N_{peak}, such that

$$\max_{z_1 \le z \le z_2} \xi_0 = \langle R_H(N_{peak}) \rangle \, . \tag{3.2}$$

For $N > N_{peak}$, the redshift range for possible absorbers is clipped, so that their number decreases. The highest accessible column density N_{cut} is reached once

$$\min_{z_1 \le z \le z_2} \xi_0 = \langle R_H(N_{cut}) \rangle \, . \tag{3.3}$$

If (min ξ_0) = 0, arbitrarily high column densities can appear, but only in an arbitrarily small number of absorbers. Therefore, the peak of $f(N)$ at $N_{\rm peak}$ is then followed by a decrease with a finite slope for higher N. If (min ξ_0) is finite, there exists a finite upper limit $N_{\rm cut}$ to the accessible column densities, where $f(N)$ is steeply cut off. The minimum value of ξ_0 can vanish if and only if $z_1 = 0$ or $z_2 = z_{\rm QSO}$, as is the case in Figure 2*a*. In all other cases, $f(N)$ is cut off at a finite column density $N_{\rm cut}$, as shown in Figure 2*b*. Moreover, since $\xi_0 \propto \sigma_v^2$, the peak location measures the velocity dispersion and thus the depth of the gravitational potential of the absorber.

In reality, the sharp peaks apparent in Figure 2 may be broadened due to possible clumpiness of the H I distribution or due to an average over different density profiles of disk galaxies of different morphological types (see Broeils & van Woerden 1994). This smoothing of the peaks may render it difficult to constrain the value of the cosmological constant just from the measured location of the peaks. It is also important to note that for high column densities, the potential obscuration of the QSOs by dust is expected to be strong and therefore should be taken into account (Fall, Pei, & McMahon 1989; Pei, Fall, & Bechtold 1991; Fall & Pei 1993). The dust obscuration tends to reduce the observed number of QSOs with high column density absorbers. Fall & Pei (1995) quantify the influence of dust on $f(N)$ by through the relation

$$f_{\rm obs}(N, z) = f_{\rm true}(N, z) \exp\left[-(b-1)k(z)\left(\frac{N}{10^{21}\ {\rm cm}^{-2}}\right)\right], \tag{3.4}$$

where $f_{\rm obs}(N, z)$ and $f_{\rm true}(N, z)$ are the observed and the true column density distributions, respectively, b is the bright-end slope of the QSO luminosity function (cf. eq. [2.31]), and $k(z)$ quantifies the redshift-dependent dust-to-gas ratio. Fall & Pei (1995) find $k(z) \approx 0.1$ at $z \approx 2$–3, which implies that disks become optically thick to dust at $\log [N({\rm cm}^{-2})] \approx 21.6$. Consequently, the curves shown in Figure 2*a* are truncated exponentially above this column density. The central opacity of nearby disk galaxies is still a subject of current debate (see, e.g., Byun 1993; Davies et al. 1993; Byun, Freeman, & Kylafis 1994; Jansen et al. 1994; Rix 1995), and the evolution of this opacity with redshift is even more uncertain. It is therefore less straightforward to assess the effect of dust on moderate-redshift absorbers. Although dust obscuration has the opposite sign to that of the magnification bias, its impact on the predicted $f(N)$ is limited because of the sharp cutoff introduced by the bending of light rays due to lensing. The dust-to-gas fraction is expected to rise as the absorber redshift decreases. However, the observed QSO light then corresponds to larger wavelengths where dust extinction is less effective. We prefer to show the unobscured $f(N)$ in Figure 2 in order to isolate the effect of lensing on the column density distribution from other effects already discussed in the literature.

The distortion of the column density distribution due to lensing affects the inferred value of the cosmological density parameter in neutral hydrogen, $\Omega_{\rm H\,I}$. Figure 3 shows the ratio between the inferred and the true value of $\Omega_{\rm H\,I}$ for two choices for the absorber–redshift interval and for the three cosmological models specified before. Similar to observational studies (e.g., Lanzetta et al. 1995), we calculate the contribution to $\Omega_{\rm H\,I}$ of damped absorption systems with $20 \le \log (N\ {\rm cm}^2) \le 22$. In Figure 3*a*, we consider the

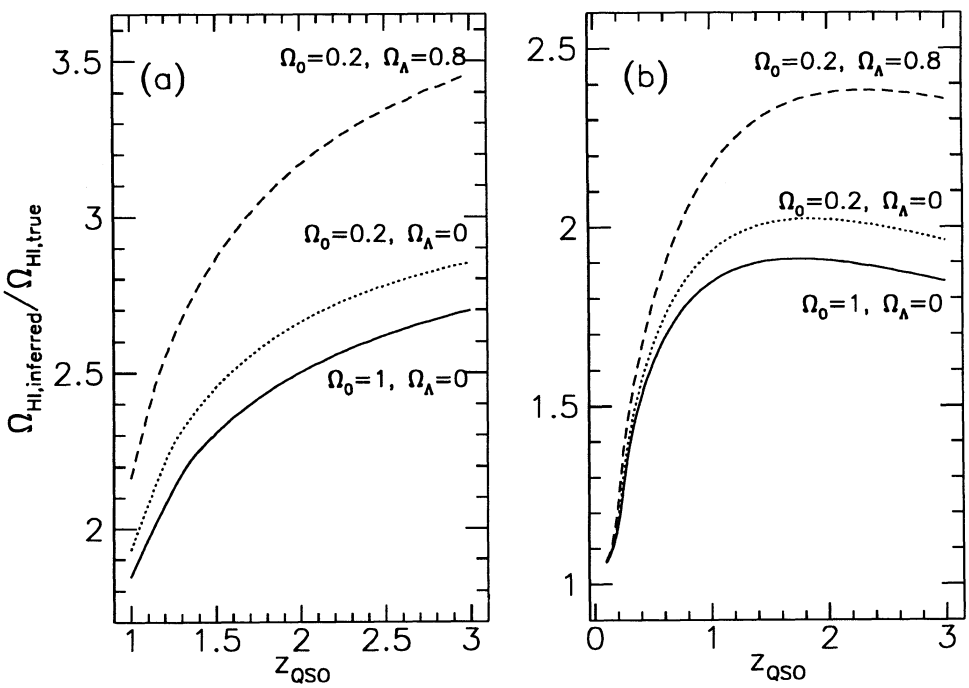

FIG. 3.—The ratio between the inferred and the true cosmological density parameter in neutral hydrogen, $\Omega_{\rm H\,I}$, is shown for two different choices of the absorber redshifts and the three cosmological models considered in Fig. 2. In (*a*), we average the result over absorber redshifts in the interval $0 \le z_{\rm abs} \le 1$, while the QSO redshift is increased from $z_{\rm QSO} = 1$ to $z_{\rm QSO} = 3$. In (*b*), the QSO redshifts range within $0 \le z_{\rm QSO} \le 3$, while the absorber redshifts lie between zero and $z_{\rm QSO}$. In both cases, the inferred density parameter decreases at low redshifts. For low QSO redshifts, $z_{\rm QSO} < 0.5$, the inferred density parameter underestimates the true H I density, but for $z_{\rm QSO} > 0.5$, the neutral hydrogen density is overestimated. A limiting QSO magnitude of $B = 17$ was assumed. For the sensitivity of the result to the QSO magnitude threshold, see Fig. 5.

absorber redshift interval $0 \leq z_{abs} \leq 1$ while the QSO redshift ranges between $1 \leq z_{QSO} \leq 3$. In Figure 3*b*, the QSO redshift varies in the range $0 \leq z_{QSO} \leq 3$, and the absorber redshifts range within $0 \leq z_{abs} \leq z_{QSO}$.

The most prominent feature in both panels is the artificial decline of the inferred value of $\Omega_{H\,I}$ with decreasing redshift, imitating a strong evolution of the neutral hydrogen density with redshift. This noticeable effect arises because $\Omega_{H\,I}$ is dominated by the high column density absorbers, for which gravitational lensing can strongly influence the result due to the magnification bias.

The discrepancies between the inferred and the true values of $\Omega_{H\,I}$ are strongest in case of a nonzero cosmological constant, as shown by the dashed curves. It is interesting that the artificial evolution in the apparent $\Omega_{H\,I}(z)$ is already comparable to that observed (White et al. 1993; Bahcall et al. 1993; Lanzetta et al. 1995), even before including any plausible amount of gas consumption by star formation (e.g., Kauffmann & Charlot 1994; Lanzetta et al. 1995). Although the observed evolution is often expressed in terms of $\Omega_{H\,I}$ as a function of z_{abs} rather than z_{QSO}, the previous searches were constrained to find high-redshift absorbers in the spectra of high-redshift QSOs (using ground-based observations) and bright low-redshift QSOs in surveys of low-redshift absorbers (using *IUE* data).

The expected redshift distribution of the damped Lyα absorption systems is presented in Figure 4, given two choices of the absorber–redshift intervals. For the curves in Figure 4*a*, $2 \leq z_{abs} \leq 3$, and for the curves in Figure 4*b*, $0 \leq z_{abs} \leq 1$. In both cases, the QSO redshift is kept fixed at $z_{QSO} = 3$. The solid curves show the result derived including lensing, while lensing was ignored for the dashed curves. Only results for the cosmological model with $\Omega_0 = 0.2$ and $\Omega_\Lambda = 0$ are shown because for this model the difference between the lensed and unlensed cases is intermediate (cf. Fig. 3). Both panels suggest that it might be difficult to distinguish between the lensed and unlensed cases on the basis of the absorber–redshift distribution alone. Especially if Ω_Λ is small, the curves are virtually indistinguishable given any reasonable error bars in the actual data. In addition, allowing for a range of QSO redshifts would tend to smear out and further reduce the difference between the two curves.

The insensitivity of the absorber–redshift distribution to lensing (cf. Fig. 4), and the weakness of the distortion of $f(N)$ due to lensing for high-redshift absorbers (cf. Fig. 2*a*), offer a plausible explanation as to why these imprints of lensing were not identified observationally in the past. The lensing signatures would be most significant in samples of bright, high-redshift QSOs which are surveyed for low-redshift, damped Lyα absorption with $z_{abs} \lesssim 1$. Unfortunately, existing surveys of damped Lyα systems (e.g., Lanzetta et al. 1995) do not include a sufficiently large number of cases with $z_{QSO} \gtrsim 2$–3 and $z_{abs} \lesssim 1$. However, it should be straightforward to design a search strategy for the purpose of detecting the lensing signature, because high column density absorbers and bright QSOs are both easy to detect.

Since the amplitude of the magnification bias depends on the QSO brightness, the inferred value of $\Omega_{H\,I}$ depends on the magnitude limit of the QSO sample. The three curves in Figure 5 show this dependence for the three cosmological models considered before. We assume $z_{QSO} = 3$ and $0 \leq z_{abs} \leq 1$. The figure shows that the value of $\Omega_{H\,I}$ can be substantially overestimated for a bright QSO sample. The dependence of $\Omega_{H\,I}$ on the magnitude limit of the QSO sample can be used to separate evolutionary effects in the absorber population from effects caused by gravitational lensing.

Figure 6 shows the fraction of all QSOs which show damped Lyα absorption with $N \geq 10^{21}$ cm^{-2} that are multiply imaged with a magnification ratio of their images $(\mu_1/\mu_2) \leq q$. The two panels display results for different absorber-redshift intervals. For

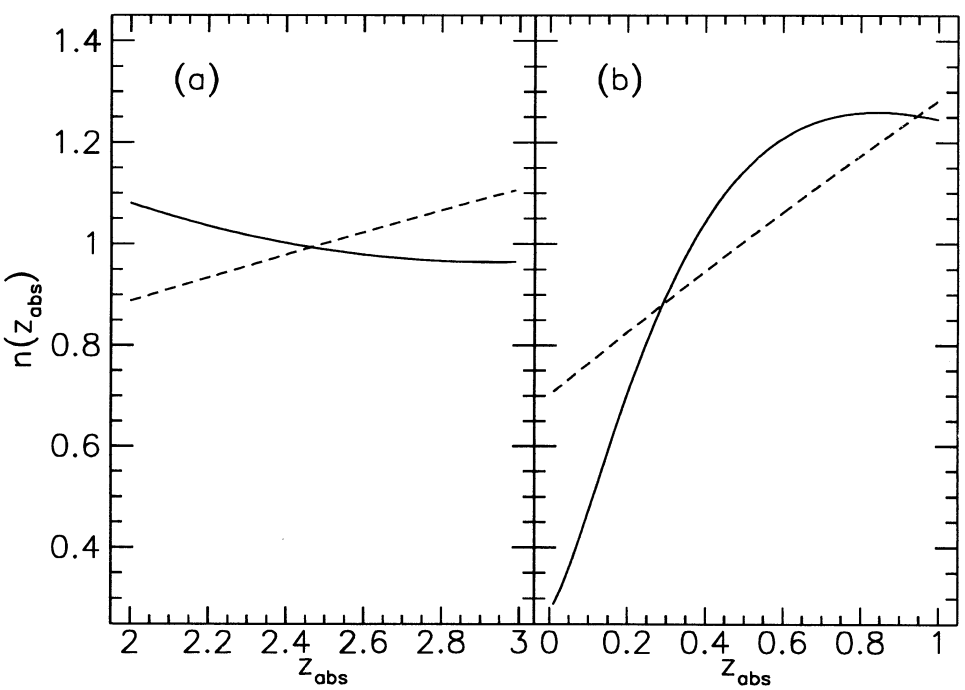

FIG. 4.—Normalized redshift distribution of damped Lyα absorbers in the spectra of QSOs at a redshift $z_{QSO} = 3$, for absorbers at either high redshifts, $2 \leq z_{abs} \leq 3$ (*a*) or low redshifts, $0 \leq z_{abs} \leq 1$ (*b*). In both panels, the dashed curve was derived ignoring gravitational lensing, while the solid curves were derived including lensing. Only results for the cosmological parameters $\Omega_0 = 0.2$, $\Omega_\Lambda = 0$ are shown. The curves are arbitrarily normalized to unit area.

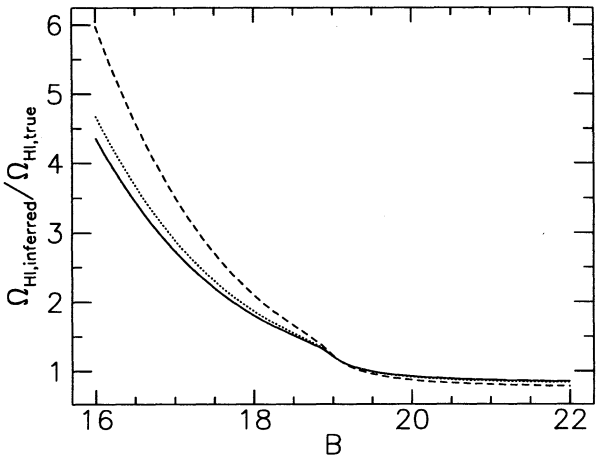

FIG. 5.—The inferred neutral hydrogen density parameter depends on the limiting magnitude B of the QSO sample due to lensing. We consider a QSO redshift $z_{QSO} = 3$ and absorbers in the redshift interval $0 \leq z_{abs} \leq 1$. The three curves show the ratio between the inferred and the true Ω_{HI} for the three cosmological models used in Fig. 2.

$2 \leq z_{abs} \leq 3$, the fraction of high column density absorbers that show double images can be used as a sensitive test for the cosmological constant. For low-redshift absorbers ($0.4 \leq z_{abs} \leq 1$), $\sim$60%–80% of all QSOs should be doubly imaged with a magnification ratio below $q = 2$. The characteristic separation between the images is $\sim$0.″3 for an L_* spiral galaxy at $z_{abs} \sim 1$. Therefore, absorbers with $N \geq 10^{21}$ cm^{-2} can be used to flag possibly lensed quasars with small image separation. Since such absorbers are easy to identify through low-resolution spectroscopy, this approach can potentially enhance the efficiency of searches for new gravitational lenses with *HST* from its present value of $\sim$1% (Bahcall et al. 1992; Maoz et al. 1993) up to several tens of percent.

4. CONCLUSIONS

The signature of gravitational lensing is particularly strong for systems that are easy to observe, namely high column density absorbers ($N \gtrsim 10^{21}$ cm^{-2}) in the spectra of bright QSOs ($B \lesssim 18$). There are five possibilities to verify the existence of lensing:

1. The apparent cosmological density of hydrogen should decline considerably toward low redshifts (cf. Fig. 3). Such a decline has, in fact, been observed (White et al. 1993; Bahcall et al. 1993; Lanzetta et al. 1995). However, the interpretation of the observed

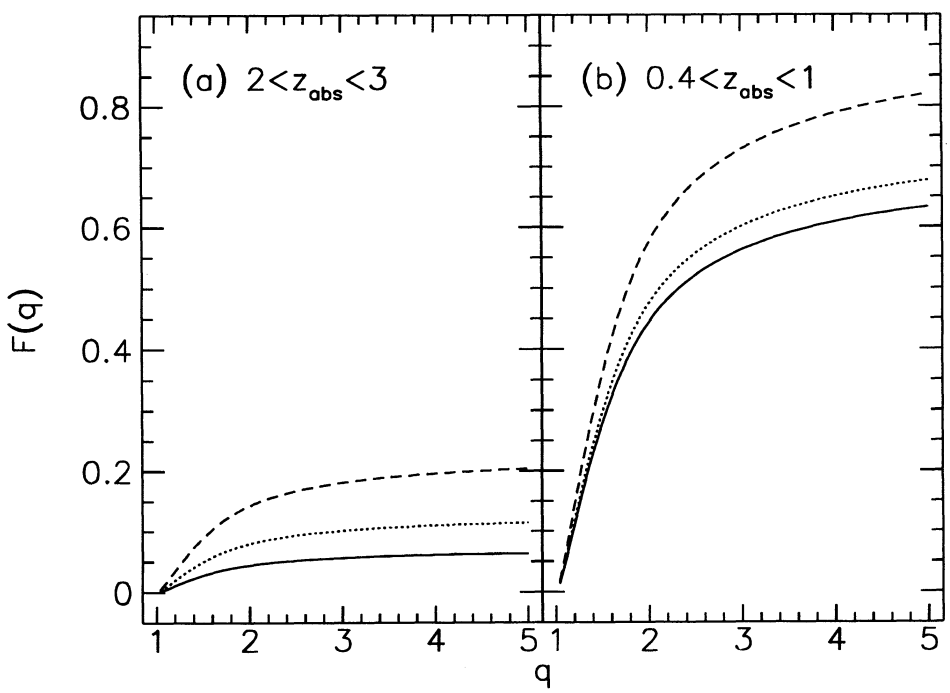

FIG. 6.—The fraction of multiple images among bright QSOs ($B \leq 17$) showing damped Lyα absorption with $N \geq 10^{21}$ cm^{-2} as a function of the maximum magnification ratio $\mu_1/\mu_2 \leq q$ of their images. In (*a*) we consider absorbers with $2 \leq z_{abs} \leq 3$, while in (*b*), $0.4 \leq z_{abs} \leq 1$. In both panels, $z_{QSO} = 3$. The different line types describe the three cosmological models considered in Fig. 2.

trend in $\Omega_{\rm H\,I}(z)$ is ambiguous because it could also result from the consumption of gas by star formation (e.g., Kauffmann & Charlot 1994; Lanzetta et al. 1995). To avoid confusion with such evolutionary effects of the damped Lyα absorber population, it is advantageous to make use of the dependences of the magnification bias on the source properties.

2. The inferred value of $\Omega_{\rm H\,I}$ should increase with increasing source luminosity (cf. Fig. 5) or source redshift (cf. Fig. 3) even if the absorber redshift interval is kept fixed. These effects cannot be imitated by an evolution of the population of damped Lyα absorbers.

3. The column density distribution for low-redshift absorbers in the spectra of high-redshift QSOs, $f(N)$, should show a pronounced peak followed by a sharp cutoff at high column densities. For QSOs brighter than $B \sim 17$ with redshifts $z_{\rm QSO} \gtrsim 2$, and for nonevolving absorbers in the redshift interval $z_{\rm abs} \sim 0.4$–1, the peak should appear around $N \sim (3\text{–}5) \times 10^{21}$ cm^{-2}. The location and height of the peak can be used to constrain the depth of the absorber potential wells or the value of the cosmological constant (cf. Fig. 2). Since $\Omega_{\rm H\,I}$ is obtained through an integral over the column density distribution of damped systems, the first two signatures listed above may be easier to probe than this third one. This could explain why the first signature may have already been observed.

4. When image splitting occurs, the absorption spectrum should show the superposition of two distinct absorption troughs corresponding to the different impact parameters of the two images. The two troughs are weighted by their corresponding image magnification factors (cf. Fig. 6). Since the equivalent width of each absorption feature scales as $N^{1/2}$, and since one of the images is usually faint, it may prove difficult to probe this spectroscopic signature.

5. High-resolution imaging of absorbers with deep potential wells may uncover the existence of multiple images. The image separation of $\sim 0\farcs3\,(v_c/220\ {\rm km\ s^{-1}})^2$ expected for $z_{\rm abs} \sim 1$ is easily detectable with *HST* unless the magnification ratio of the images is extreme. The fraction of doubly imaged QSOs that show damped Lyα absorption with $N \geq 10^{21}$ cm^{-2} ranges from $\sim 10\%$ for $2 \leq z_{\rm abs} \leq 3$ up to 80% for $0.4 \leq z_{\rm abs} \leq 1$ (cf. Fig. 6). Therefore, strong damped Lyα systems may serve as reliable flags for lensed QSOs with small image splitting. The identification of such systems requires only low-resolution spectroscopy. The selection of bright QSOs which are known to have strong damped Lyα absorption lines may then be used to enhance the efficiency of searches for new gravitational lenses with *HST* (cf. Maoz et al. 1993).

6. Since the magnification bias is strongest for high column density systems which arise mainly from highly inclined disks, strong Faraday rotation should be frequent in lenses which are damped Lyα absorbers.

As in any other astrophysical study, there are various factors that may complicate the analysis of observational data. First, obscuration by dust may hide the lensed images of a QSO. The abundance of dust in damped Lyα systems can be inferred from the reddening of the background QSOs. A comparison between the spectra of QSOs with and without damped Lyα systems implies that the most likely dust-to-gas ratio in damped Lyα systems at $z_{\rm abs} \gtrsim 2$ is only 5%–20% of the Milky Way value (Fall et al. 1989; Pei et al. 1991; Fall & Pei 1993, 1995). This estimate is supported by the observed abundances of Zn and Cr in the absorbers (e.g., Sembach et al. 1995, and references therein). Therefore, the high-redshift absorbers are expected to be optically thin for H I column densities $\lesssim 10^{21.6}$ cm^{-2} (cf. eq. [3.4]). Although the dust content of low-redshift absorbers could be higher than that, their obscuration is related to the low-extinction part of the dust extinction curve in the V band, where most QSO surveys are done. At low redshifts, the effect of dust can be readily corrected for by using the inferred obscuration profiles of nearby disk galaxies (e.g., Byun 1993; Byun et al. 1994; Jansen et al. 1994; Rix 1995), but these are still a matter of current debate.

Note that the bending of light rays from the source due to lensing tends to weaken the effect of dust as it provides a minimum impact parameter, of order ~ 1–2 kpc, for the bright image of the QSO. Thus, if dust obscuration is strong in the inner part of damped Lyα absorbers, then the significance of lensing may be emphasized even more, because without lensing fewer QSOs would have been seen behind the center of the absorber. Aside from adding QSOs through the magnification bias, the ray bending due to lensing brings additional QSOs into view that would otherwise be hidden behind a thicker layer of dust.

In this study, we have concentrated on the effect of gravitational lensing *relative* to the case when lensing is neglected. Therefore, some of our conclusions are independent of the effects of dust. For example, when double images occur, both of them are likely to be observed because for common magnification ratios ($q \lesssim 2$), the images appear at comparable impact parameters with similar dust extinction. Of course, dust can change the *absolute* numbers derived from the statistics of damped Lyα systems.

A second complication to our analysis involves possible clumpiness of the H I distribution in the absorbers. Clumpiness would tend to broaden the distribution of column densities at a given impact parameter beyond the geometric spread induced by different inclinations. This effect would then broaden the peaks shown in Figure 2. An argument against the existence of strong ($\gtrsim 30\%$) clumpiness on small scales ($\lesssim 1$–2 kpc) is provided by the similarity between the column densities observed in the two images of the lensed QSO 0957+561 at $z_{\rm QSO} = 1.41$; the separate lines of sight corresponding to the two images cross a common damped Lyα absorber at $z_{\rm abs} = 1.391$ and show a similar column density in their spectra (Turnshek & Bohlin 1993). Locally, however, Kamphuis, Sancisi, & van der Hulst (1991) have found a remarkable H I "bubble" in M101. In general, the higher the overdensity of the H I clumps, the smaller is their cross section and the less likely they are to appear in absorption spectra. Clumpiness should be less important for estimates of averaged quantities such as $\Omega_{\rm H\,I}$ than for differential quantities like $f(N)$.

Finally, a third complication to our modeling may arise from possible evolution in the properties of the absorbers. If the observed H I disks are much bigger at high redshift, then for a given H I column density the characteristic impact parameter increases and the lensing signatures are weakened relative to our no-evolution model. However, it should be easy to disentangle the pure lensing effect from any such evolutionary effect by examining the second signature mentioned above. We address the above three complications in a future paper (Perna, Loeb, & Bartelmann 1996).

Recently, there has been considerable interest in the cosmological abundance of damped Lyα systems as a means of constraining variants of cold dark matter cosmologies, such as the mixed dark matter (MDM) model, in which galaxies form relatively late (Klypin et al. 1995; Kauffmann & Charlot 1994; Ma & Bertschinger 1994; Mo & Miralda-Escudé 1994). The magnification bias derived in this paper should in general be incorporated into those studies. In addition, the observed sample of absorbers may be

biased toward higher velocity dispersion σ_v because the magnification bias depends strongly on σ_v. However, this effect is limited by the exponential cutoff of the Schechter luminosity function.

Some of the gravitational lensing signatures listed above were not discovered observationally in the past due to an unfortunate combination of selection effects. Ground-based observations were limited to absorbers at high redshift, while *IUE* observations (Lanzetta et al. 1995) focused on low-redshift sources. In both cases the signature of lensing was artificially minimized by the lensing geometry. Forthcoming observations with *HST* could easily detect a few of the above five signatures if properly designed. The search strategy should focus on finding high column density ($N \gtrsim 10^{21}$ cm^{-2}) absorbers in the spectra of bright ($B \lesssim 16$–17), high-redshift ($z_{QSO} \gtrsim 2$–3) QSOs. Detection of the peaks shown in Figure 2 or the fraction of multiply imaged QSOs shown in Figure 6 may be possible in a sample of more than 10 damped Lyα systems with $N \gtrsim 10^{21}$ cm^{-2} and $0.5 \lesssim z_{abs} \lesssim 1$. Quantitative measurement of these and the other lensing signatures can be used to constrain the gravitational potential depth of the absorbers and the cosmological constant.

There is one known gravitational lens system, B0218+357, which is an almost perfect example for the case we make in this paper. The source was discovered in the radio and found to be an Einstein ring with two compact components (O'Dea et al. 1992; Patnaik et al. 1993). Evidence that the lens is a spiral galaxy comes from the small radius of the Einstein ring, $\sim 0\farcs3$, the occurrence of Hβ and [O III] λ5007 emission which are common features of late-type spirals (Browne et al. 1993), the existence of 21 cm absorption by neutral hydrogen at the same redshift ($z_{abs} = 0.68$) as the optical emission lines (Carilli et al. 1993), and the presence of strong Faraday rotation with a rotation measure of ~ 3000 rad m^{-2} (Patnaik et al. 1993). The observed 21 cm absorption implies an H I column density of $N = 4 \times 10^{21}$ cm^{-2} $(T_s/100\ \mathrm{K})/(f/0.1)$, where T_s is the spin temperature of the gas and f is the H I covering factor. The source shows a featureless BL Lacertae–type spectrum (O'Dea et al. 1992) and is red in the optical, probably due to the influence of dust (Grundahl & Hjorth 1995). We expect systems similar to B0218+357 to be frequent among QSOs showing strong damped Lyα absorption.

We wish to thank Emilio Falco, Michael Fall, Chris Kochanek, Jordi Miralda-Escudé, Yi-Chuan Pei, Joel Primack, Hans-Walter Rix, and Peter Schneider for useful remarks, and especially the referee, Ed Turner, for his constructive comments. M. B. was supported in part by the Sonderforschungsbereich SFB 375-95 of the Deutsche Forschungsgemeinschaft.

Note added in manuscript: After the completion of this work, we became aware that a related study had been performed by Smette et al. (1995). In addition, Ed Turner emphasized to us the potential effect of a finite core on the predictions from our singular lens model. Although this effect may not have drastic consequences (cf. Fig. 3*a* of Kochanek & Blandford 1987), we intend to address it in detail, together with the effects of dust obscuration, in a forthcoming publication (Perna et al. 1996).

REFERENCES

Aaronson, M., Huchra, J., & Mould, J. 1979, ApJ, 229, 1
Bahcall, J. N., et al. 1993, ApJS, 87, 1
Bahcall, J. N., Maoz, D., Schneider, D. P., Yanny, B., & Doxsey, R. 1992, ApJ, 392, L1
Bahcall, J. N., & Peebles, P. J. E. 1969, ApJ, 156, L7
Boyle, B. J., Shanks, T., & Peterson, B. A. 1988, MNRAS, 235, 935
Briggs, F. H., Wolfe, A. M., Liszt, H. S., Davis, M. M., & Turner, K. L. 1989, ApJ, 341, 650
Broeils, A. H., & van Woerden, H. 1994, A&AS, 107, 129
Browne, I. W. A., Patnaik, A. R., Walsh, D., & Wilkinson, P. N. 1993, MNRAS, 263, L32
Burbidge, G., Odell, S. L., Roberts, D. H., & Smith, H. E. 1977, ApJ, 218, 33
Byun, Y. I. 1993, PASP, 105, 993
Byun, Y. I., Freeman, K. C., & Kylafis, N. D. 1994, ApJ, 432, 114
Carilli, C. L., Rupen, M. P., & Yanny, B. 1993, ApJ, 412, L59
Davies, J. I., Phillipps, S., Boyce, P. J., & Disney, M. J. 1993, MNRAS, 260, 491
Fall, S. M., & Pei, Y. C. 1993, ApJ, 402, 479
———. 1995, in Proc. ESO: Workshop on QSO Absorption Lines, ed. G. Meylan, in press
Fall, S. M., Pei, Y. C., & McMahon, R. G. 1989, ApJ, 341, L5
Grundahl, F., & Hjorth, J. 1995, SISSA preprint astro-ph/9506085
Hartwick, F. D. A., & Schade, D. 1990, ARA&A, 28, 437
Holmberg, E. B. 1975, in Galaxies and the Universe, ed. A. Sandage, M. Sandage, & J. Kristian (Chicago: Univ. of Chicago Press), 151
Ikeuchi, S., & Turner, E. L. 1991, ApJ, 375, 499
Jansen, R. A., Knapen, J. H., Beckman, J. E., Peletier, R. F., & Hes, R. 1994, MNRAS, 270, 373
Kamphuis, J., Sancisi, R., & van der Hulst, T. 1991, A&A, 244, L29
Kauffmann, G., & Charlot, S. 1994, ApJ, 430, L97
Klypin, A., Borgani, S., Holtzman, J., & Primack, J. 1995, ApJ, 444, 1
Kochanek, C. S. 1991, ApJ, 373, 354
———. 1992, ApJ, 384, 1
Kochanek, C. S., & Blandford, R. D. 1987, ApJ, 321, 676
Krolik, J. H., & Kwan, J. 1979, Nature, 281, 520
Kronberg, P. P., Perry, J. J., & Zukowski, E. L. H. 1992, ApJ, 387, 528
Lanzetta, K. M., & Bowen, D. V. 1992, ApJ, 391, 48
Lanzetta, K. M., Wolfe, A. M., & Turnshek, D. A. 1995, ApJ, 440, 435
Lanzetta, K. M., Wolfe, A. M., Turnshek, D. A., Lu, L., McMahon, R. G., & Hazard, C. 1991, ApJS, 77, 1
Lu, L., & Wolfe, A. M. 1994, AJ, 108, 44
Lu, L., Wolfe, A. M., Turnshek, D. A., & Lanzetta, K. M. 1993, ApJS, 84, 1
Ma, C.-P., & Bertschinger, E. 1994, ApJ, 434, L5
Maoz, D., et al. 1993, ApJ, 409, 28
Marzke, R. O., Geller, M. J., Huchra, J. P., & Corwin, H. G., Jr. 1994, AJ, 108, 437
Mo, H. J., & Miralda-Escudé, J. 1994, ApJ, 430, L25
Narayan, R., & Wallington, S. 1993, in Proc. 31st Liège Astrophys. Coll., Gravitational Lenses in the Universe, ed. J. Surdej et al. (Liège: Université de Liège), 217
O'Dea, C. P., Baum, S. A., Stanghellini, C., Dey, A., van Breughel, W., Deustua, S., & Smith, E. 1992, AJ, 104, 3120
Patnaik, A. R., Browne, I. W. A., King, L. J., Muxlow, T. W. B., Walsh, D., & Wilkinson, P. N. 1993, MNRAS, 261, 435
Peebles, P. J. E. 1993, Principles of Physical Cosmology (Princeton: Princeton Univ. Press)
Pei, Y. C. 1995, ApJ, 438, 623
Pei, Y. C., Fall, S. M., & Bechtold, J. 1991, ApJ, 378, 6
Perna, R., Loeb, A., & Bartelmann, M. 1996, in preparation
Perry, J. J., Watson, A. M., & Kronberg, P. P. 1993, ApJ, 406, 407
Peterson, B. M., Strom, S. E., & Strom, K. M. 1979, AJ, 84, 735
Pettini, M., Smith, L. J., Hunstead, R. W., & King, D. L. 1994, ApJ, 426, 79
Rix, H.-W. 1995, in Proc. NATO Advanced Research Workshop, Opacity of Spiral Disks (Cardiff, 1994 July), ed. J. Davies, in press
Rix, H.-W., Schneider, D. P., & Bahcall, J. N. 1992, AJ, 104, 959
Schechter, P. 1976, ApJ, 203, 297
Schneider, P. 1992, A&A, 254, 14
Schneider, P., Ehlers, J., & Falco, E. E. 1992, Gravitational Lenses (Heidelberg: Springer)
Sembach K. R., Steidel, C. C., Macke, R. J., & Meyer, D. M. 1995, ApJ, 445, L27
Smette, A., Claeskens, J., & Surdej, J. 1995, in IAU Symp. 173, Astrophysical Applications of Gravitational Lensing, ed. C. S. Kochanek & J. N. Hewitt (Kluwer: Academic), in press
Steidel, C. C., Bowen, D. V., Blades, J. C., & Dickinson, M. 1995, ApJ, 440, L45
Steidel, C. C., Pettini, M., Dickinson, M., & Persson, S. E. 1994, AJ, 108, 2046
Storrie-Lombardi, L. J., McMahon, R. G., Irwin, M. J., & Hazard, C. 1995, in Proc. ESO Workshop on QSO Absorption Lines, ed. G. Meylan, in press
Strauss, M. A., & Willick, J. A. 1995, Phys. Rep., in press
Thomas, P. A., & Webster, R. L. 1990, ApJ, 349, 437
Tóth, G., & Ostriker, J. P. 1992, ApJ, 389, 5
Tremaine, S. 1996, in preparation
Tully, R. B., & Fisher, J. R. 1977, A&A, 54, 661
Turner, E. L. 1990, ApJ, 365, L43
Turnshek, D. A., & Bohlin, R. C. 1993, ApJ, 407, 60

Turnshek, D. A., Wolfe, A. M., Lanzetta, K. M., Briggs, F. H., Cohen, R. D., Foltz, C. B., Smith, H. E., & Wilkes, B. J. 1989, ApJ, 344, 567
Tytler, D. 1987, ApJ, 321, 49
Welter, G. L., Perry, J. J., & Kronberg, P. P. 1984, ApJ, 279, 19
White, R. L., Kinney, A. L., & Becker, R. H. 1993, ApJ, 407, 456
Wolfe, A. M. 1988, in QSO Absorption Lines: Probing the Universe, ed. J. C. Blades, D. A. Turnshek, & C. A. Norman (Cambridge: Cambridge Univ. Press), 297
Wolfe, A. M., Lanzetta, K. M., & Oren, A. L. 1992 ApJ, 388, 17
Wolfe, A. M., Turnshek, D. A., Lanzetta, K. M., & Lu, L. 1993, ApJ, 404, 480
Wolfe, A. M., Turnshek, D. A., Lanzetta, K. M., & Oke, J. B. 1992, ApJ, 385, 151
Wolfe, A. M., Turnshek, D. A., Smith, H. E., & Cohen, R. D. 1986, ApJS, 61, 249
Zaritsky, D. 1995, ApJ, 448, L17